



Promoting repair of highly purified stromal vascular fraction gel combined with advanced platelet-rich fibrin extract for irradiated skin and soft tissue injury

Zhou Li^{1#}, Huimin Gan^{1#}, Anru Liang^{2,3}, Xiyue Wang⁴, Xiaohao Hu⁴, Ping Liang¹, Guoding Xu¹, Qianwen Huang⁵, Junjun Li⁶, Hongmian Li⁷

¹Department of Oncology, The Fifth Affiliated Hospital of Guangxi Medical University, Nanning, China; ²Department of Plastic Surgery, The Third Affiliated Hospital of Guangxi Medical University, Nanning, China; ³Guangxi Kangjiu Biotechnology Co., Ltd., Nanning, China; ⁴Collaborative Innovation Centre of Regenerative Medicine and Medical BioResource Development and Application, Guangxi Medical University, Nanning, China; ⁵Nanning Wilking Biotechnology Co., Ltd., Nanning, China; ⁶Department of Pediatrics, The People's Hospital of Guangxi Zhuang Autonomous Region & Institute of Hospital Management and Medical Prevention Collaborative Innovation, Guangxi Academy of Medical Sciences, Nanning, China; ⁷Department of Plastic and Reconstructive Surgery, The People's Hospital of Guangxi Zhuang Autonomous Region & Research Center of Medical Sciences, Guangxi Academy of Medical Sciences, Nanning, China

Contributions: (I) Conception and design: H Li, J Li; (II) Administrative support: Q Huang, G Xu, P Liang; (III) Provision of study materials or patients: Z Li, H Gan, A Liang, X Wang; (IV) Collection and assembly of data: Z Li, X Wang; (V) Data analysis and interpretation: X Wang, X Hu; (VI) Manuscript writing: All authors; (VII) Final approval of manuscript: All authors.

[#]These authors contributed equally to this work.

Correspondence to: Hongmian Li. Department of Plastic and Reconstructive Surgery, The People's Hospital of Guangxi Zhuang Autonomous Region & Research Center of Medical Sciences, Guangxi Academy of Medical Sciences, Nanning 530021, China. Email: lihongmian@gxmu.edu.cn; Junjun Li. Department of Pediatrics, The People's Hospital of Guangxi Zhuang Autonomous Region & Institute of Hospital Management and Medical Prevention Collaborative Innovation, Guangxi Academy of Medical Sciences, Nanning 530021, China. Email: lijunjun6225@163.com.

Background: To evaluate the effect of highly purified stromal vascular fraction gel (SVFG) combined with advanced platelet-rich fibrin extract (APRFE) in treatment of irradiated skin and soft tissue injury.

Methods: The subcutaneous fat and whole blood of 4 rabbits were collected to isolate the SVFG and APRFE, respectively. Forty-eight rabbits were divided into 4 groups to prepare irradiated skin injury models with 25 Gy for 24 hours; corresponding dose were performed subcutaneously injected into wounds. In group A, the rabbits were treated with 0.3 mL APRFE combined with 1 mL SVFG. In group B, the rabbits were treated with 1 mL SVFG. In group C, the rabbits were treated with 0.3 mL APRFE, and group D was treated with 1 mL normal saline. The wound healing was detected on the 2, 5, 9 and 14 d after intervention. The wounds tissue was cut for hematoxylin and eosin (HE) staining to observe the structure and Masson staining to observe the collagen content. The expression of CD31 in each group was detected by immunohistochemistry (IHC), the protein and mRNA levels of K19, hypoxia inducible factor-1 alpha (HIF-1 α), vascular endothelial growth factor (VEGF), interleukin 8 (IL-8) and interleukin 10 (IL-10) were detected respectively by Western blot (WB) and reverse transcription-polymerase chain reaction (RT-PCR) on 7, 14 and 28 d after intervention.

Results: It is revealed that wound healing rates from 5 to 14 d in group A was significantly higher than that of control. The wounds healing rates in group B and C were significantly higher than that of control after 12 d. Masson staining results showed that the collagen content in group A was significantly higher than that of the other 3 groups on the 7, 14 and 28 d. The results of IHC showed that the expression of CD31 in group A was significantly higher than that of the other 3 groups on 7, 14 and 28 d. WB and RT-PCR results showed that relative expression levels of K19, HIF-1 α , VEGF, IL-10 in group A were significantly higher than that of the other 3 groups on 7, 14 and 28 d. However, the relative expression levels of IL-8 in group A was significantly lower than that of the other 3 groups on 7, 14 and 28 d.

Conclusions: SVFG combined with APRFE can promote the repair of irradiated skin and soft tissue

injury by accelerating angiogenesis, promoting collagen synthesis and reducing inflammation.

Keywords: Stromal vascular fraction gel (SVFG); advanced platelet-rich fibrin extract (APRFE); radiation damage; skin and soft tissue; regeneration and repair

Submitted Jul 12, 2022. Accepted for publication Sep 08, 2022.

doi: 10.21037/atm-22-3956

View this article at: <https://dx.doi.org/10.21037/atm-22-3956>

Introduction

According to the Global Cancer Report of 2022, more than 4.5 million new cases of cancer were diagnosed in China in 2020 (1). More than half of all cancer patients require radiotherapy (2); which is playing an increasingly significant role in the treatment of cancer. However, tumor radiotherapy inevitably causes the surrounding normal tissue damage, skin and soft tissue damage is the most common. Following radiotherapy, mild to severe skin reactions occur in 95% of patients. Acute injuries induced by ray is characterized by skin erythema, desquamation, ulceration, hemorrhage, and necrosis. Chronic injuries induced by ray shows skin atrophy, alopecia and vascular dilation (3,4). Different from the conventional skin and soft tissue injury, the irradiated skin and soft tissue injury can lead to delayed cancer treatment, reduced patient's quality of life, and even endanger the patient's life in severe cases. These factors bring great pain to patients and their families. Therefore, it is very important to prevent and treat irradiated skin and soft tissue injury. The key to the treatment of irradiated skin and soft tissue injury is to improve the regenerative ability of the injured skin (5). Currently, many drugs and wound dressings are used to prevent and treat skin injury induced by ray. However, the consistently effective treatment and prevention strategy is lacking (6). Adipose-derived stem cells (ADSCs) have been widely used in the field of tissue repair therapy and regenerative medicine due to the advantages of easy collection, large amount of access, less damage to the body, low immunogenicity, no ethical problems, multi-differentiation and secretion of multiple cytokines (7-11). Stromal vascular fraction (SVF) is a colloidal fat derivative which obtained by physical and mechanical fragmentation following centrifugal extraction of adipose tissue, which contains not only ADSCs but also a variety of growth factors and stromal cells (12,13). stromal vascular fraction gel (SVFG), derived from fat, facilitates a new direction for the treatment of intractable wounds (14). Modified advanced

platelet-rich fibrin (APRF) is an improved production of PRF, which was obtained by increasing the time and reducing the speed of centrifugation (15). It has been found that APRF is a better carrier for a variety of growth factors, immunomodulators, platelets, and blood cells, which can effectively promote wounds healing and tissue repair (16-18). Moreover, APRF gel can be refrigerated at 4 °C for 1 week and then further produce APRF extract (APRFE). In recent years, many researchers have applied SVFG and PRF in wound healing and other regenerative medicine studies (19-23); however, the application of SVFG combined with APRFE in the treatment of irradiated skin injury has not yet been reported. Therefore, in this study, we intended to evaluate the curative effect of SVFG combined with APRFE by subcutaneously injecting a certain proportion of this complex for the treatment of irradiated skin injury and to explore the relevant mechanism, with the goal of providing new ideas and strategies for the clinical treatment of irradiated injury of the skin. We present the following article in accordance with the ARRIVE reporting checklist (available at <https://atm.amegroups.com/article/view/10.21037/atm-22-3956/rc>).

Methods

Experimental animals

A total of 52 male healthy SPF adult New Zealand rabbits aged 80 days and weighing approximately 2±0.2 kg (Wuxi Hengtai Experimental Animal Breeding Co., Wuxi, China) were selected. Four of those were used to separate SVFG and 48 were used for SVFG and APRFE intervention.

Ethical statement

Animal experiments were performed under a project license (No. 2020-106-01) granted by the Ethics Committee of the Fifth Affiliated Hospital of Guangxi Medical University, in

compliance with the institutional guidelines for the care and use of animals. A protocol was prepared before the study without registration.

Experimental reagents and instruments

The following list of experimental reagents were used: osteogenesis induction fluid (Wuxi Puhe Biotechnology Co., Ltd., Wuxi, China), 4% gelatin, 1% alizarin red (pH 4.2), ethanol, cartilage formation induction solution (Wuxi Puhe Biotechnology Co., Ltd.), oil red O dye, toluidine blue (pH 2.5; Solarbio, Beijing, China), PRF gel precipitation solution (Wuxi Puhe Biotechnology Co., Ltd.), platelet-derived growth factor (PDGF)-BB enzyme-linked immunosorbent assay (ELISA) Kit (BioSH 72328), vascular endothelial growth factor (VEGF) ELISA kit (BioSH 72257), fibroblast growth factor (FGF)-2 kit (BioSH 72329), interleukin 8 (IL-8) kit (BioSH 72066), interleukin 10 (IL-10) kit (BioSH 72056), hematoxylin (Shanghai Zhanyun Chemical Co., Ltd., Shanghai, China), eosin (Shanghai Zhanyun Chemical Co., Ltd.), neutral gum (Shanghai Yiyang Instrument Co., Ltd., Shanghai, China), Masson staining kit (Solarbio), 0.1% Triton X-100, 3% H₂O₂/phosphate-buffered saline (PBS), antigen repair solution, 3,3'-diaminobenzidine (DAB) staining kit (ZLi-9018; Zhongshan Jinqiao, Beijing, China), total RNA extraction kit (Shanghai Yudo Biotechnology Co., Ltd., Shanghai, China), SYBR Green PCR Kit (-415XL, Thermo Fisher Scientific, Waltham, MA, USA), and reverse transcription kit (#K1622, Thermo Fisher Scientific).

The following experimental instruments were used: biological X-ray irradiator (Panasonic, Tokyo, Japan), electrophoretic apparatus (Mini-PROTEAN 3 Cell, Bio-Rad Laboratories, Inc., Hercules, CA, USA), electro transducer (PS-9, Dalian Kingmai Technology Co., Ltd., Dalian, China), enzyme marker (MK3, ThermoFisher Scientific), ChemiScope 5300 Pro (Clinx, Shanghai, China), cryogenic centrifuge (Eppendorf 5417R), and a real-time detector (ABI-7500, Thermo Fisher Scientific).

Experimental methods

Isolation and identification of highly purified SVFG

Four rabbits were anesthetized to death by injection of 10% chloral hydrate; about 40 mL subcutaneous adipose tissue the rabbits was taken out of back, scapula, neck and groin. After shredded, the fat was repeatedly injected into the chylous shape with a 20 mL syringe. The treated chylous

fat was centrifuged with 2,000 g centrifugal force for 5 minutes at room temperature. A small amount of swelling fluid in the lower layer and a large amount of yellow transparent oil in the upper layer were discarded. The viscous gel-like substance under the oil layer was SVFG. The prepared SVFG was inoculated into culture dish, and the morphology of the cells was observed and photographed by inverted microscope at day 1, 3, 5, 7 and 9 respectively. Osteogenesis, adipogenesis and chondrogenesis were induced and identified respectively.

Extraction, preparation, and detection of APRFE

The aorta and heart blood of the above four rabbits were extracted at the same time, totaling about 20 mL. Then, the blood was immediately centrifuged at 1,500 rpm for 14 min. After centrifugation, three layers were formed in the centrifuge tube, the lowest layer was red blood cell layer, the surface layer was transparent and clear supernatant, and the APRF gel was located in the middle layer of the Centrifugal product, which is stored at 4 °C. The gel precipitate, namely APRFE was collected at 1, 3, 5 and 7 d, and the indexes of APRFE at each time point were detected by ELISA.

Establishing model of irradiated skin and soft tissue injury in rabbits

Twelve rabbits were randomly divided into four groups, and chloral hydrate was injected into each group according to 400 mg/kg. After anesthesia, different dose (15, 20, 25, 30 Gy) was irradiated according to the dose of 6 MeV electron beam in each group (dose rate was 300 mu/min × 12 min = 3,500 mu). After 24 hours of irradiation, pictures were taken, the healing rate of each group was recorded to select the best radiation dose.

Forty-eight rabbits were randomly divided into four groups with 12 rabbits in each group. Group A: 0.3 mL APRFE + 1 mL SVFG combined intervention group; group B: 1 mL SVFG intervention group; group C: 0.3 mL APRFE intervention group; group D: 1 mL normal saline control group. The rabbits in each group were anesthetized by intramuscular injection of chloral hydrate according to 400 mg/kg and each rabbit was irradiated with the best dose. Twenty-four hours after irradiation, the wounds were photographed and observed. According to the group, the APRFE and SVFG were subcutaneously injected into the four quadrants of the irradiated site respectively, and the changes of the wounds were observed for one to four weeks after injection. Part of the skin tissue from the irradiation

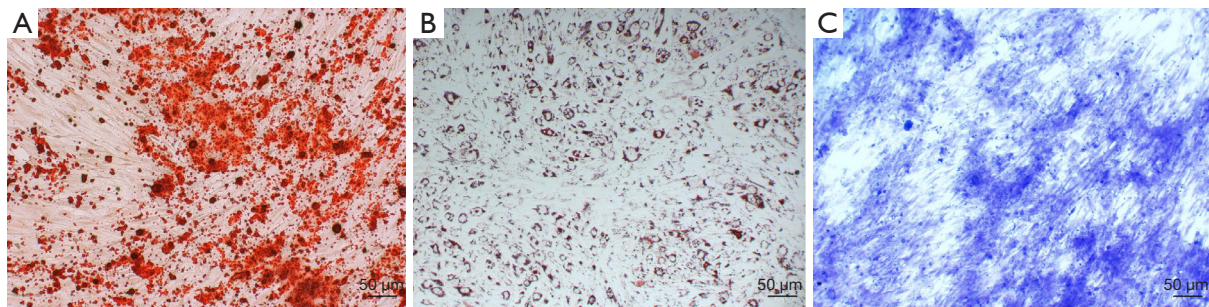


Figure 1 Identification of SVFG after induced culture 2 weeks respectively. (A) Positive alizarin red staining after 2 weeks of osteogenic induction. (B) Positive oil red O staining after 2 weeks of adipogenic induction. (C) Positive Alcian blue staining after 2 weeks of chondrogenic induction. Amplify $\times 100$. SVFG, stromal vascular fraction gel.

center was taken for subsequent experiments at 7, 14 and 28 days after irradiation, and the wound recovery was recorded.

Samples for corresponding detection

The skin tissue of the above 4 groups were sampled at 7-, 14-, and 28-day post-irradiation, and hematoxylin and eosin (HE) staining was performed. The changes of skin layers among different groups were observed and compared under microscope. Masson staining was used to observe the collagen content, and immunohistochemistry (IHC) was used to detect expression of CD31. The expression levels of protein and mRNA from the wound tissues of the above groups were detected by Western blot (WB) analysis and reverse transcription-polymerase chain reaction (RT-PCR) analysis.

Statistical analysis

The statistical software SPSS 22.0 (IBM Corp., Armonk, NY, USA) was used for statistical analysis. The measurement data were expressed as mean \pm standard deviation (SD). The differential analysis of the total mean of each group was performed by complete random design variance analysis, and pairwise multiple comparison was performed using Duncan method, with the test level $\alpha=0.05$ (bilateral).

Results

Identification of SVFG and cytokine levels measure of APRFE

After primary cells were cultured for 24 to 48 hours, a few fibroblast-like cells had adhered to the walls; most of the

unattached cells were globular. As the culture continued, the adherent cells grew in colonies of different sizes. The cells in the colonies were typical fusiform cells. After 10–12 days, the cells had formed an 80–90% confluent monolayer. The cells in the colonies were typical spindle cells. Alizarin red staining after SVFG osteogenic induction indicated significant calcified nodules formation. Oil red O staining after lipid induction revealed many lipid droplets formation. Toluidine blue staining after chondrogenic induction indicated blue tubercles aggregation (*Figure 1*).

There was no significant change of IL-8 level in 7 days. The secretory level of IL-10, VEGF and FGF-2 increased slowly from 1 to 7 days. PDGF-BB levels decreased on the 1st-5th day and increased significantly on the 7th day. Levels of IL-8, IL-10, VEGF, FGF-2 and PDGF-BB derived from the PRF membrane at different timepoints are shown in *Figure 2*.

Identification of the optimal radiation dose

The results showed that the skin was damaged severely after being irradiated by 30 Gy, and the damage reduced substantially with the lower exposure dose, from 25 to 15 Gy. The optimal exposure dose of 25 Gy was selected for subsequent experiments (*Figure 3A*).

General observation and comparison of wounds healing

We recorded the wound status with photos on the 7, 14 and 28 d after intervention (*Figure 3B*). The wounds indicated no significant differences between the 4 groups before 7 days. On day 14 and 28, the healing rate of SVFG combined with APRFE group was higher than that of the control group (*Figure 3B*). There was no significant

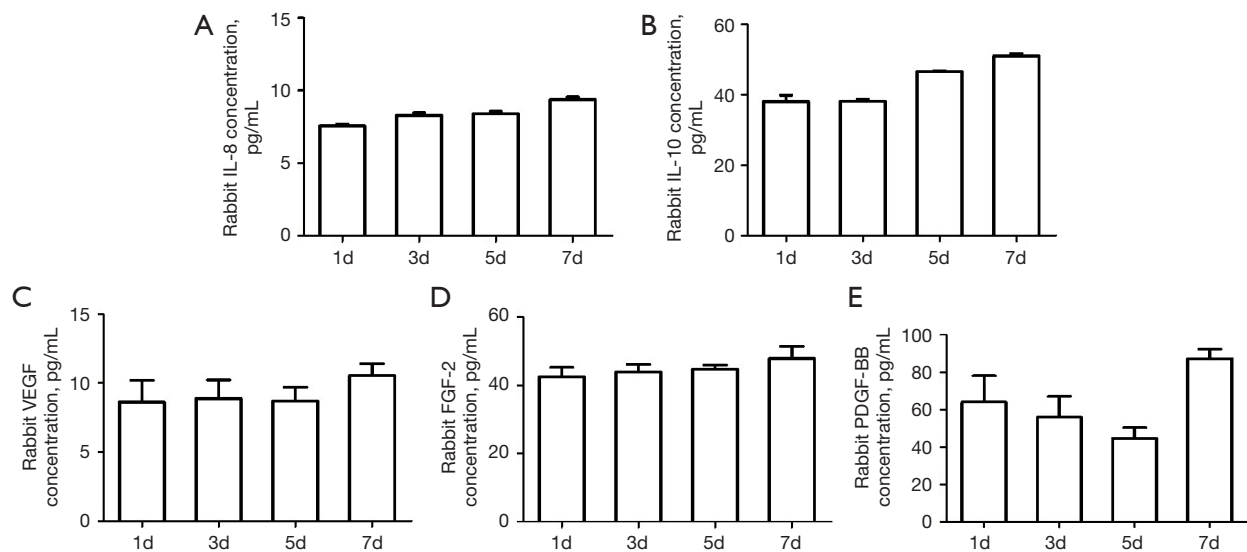


Figure 2 The levels of each cytokine in APRFE was analyzed by ELISA assay. (A) The change of IL-8 was not obvious on the 1–7 day; (B) level of IL-10 increased slowly on the 1–7 day; (C) level of VEGF increased slowly on the 1–7 day; (D) level of FGF-2 increased slowly on the 1–7 day; (E) PDGF-BB levels decreased on the 1st–5th day and increased significantly on 5–7 day. IL-8, interleukin 8; IL-10, interleukin 10; VEGF, vascular endothelial growth factor; FGF, fibroblast growth factor; PDGF, platelet-derived growth factor; APRFE, advanced platelet-rich fibrin extract; ELISA, enzyme-linked immunosorbent assay.

difference in the wound healing rate among 4 groups in the first 5 days. The healing rate of the SVFG combined with APRFE group was significantly higher than that of the control group from day 5 to 14. The healing rate of the SVFG group and APRFE groups were significantly higher than that of the control group from 12 to 14 d ($*P<0.05$, $**P<0.01$, compared with the control group, *Figure 3C*).

HE staining of wounds tissue

On 7 d after intervention, the epidermal layer of the control group was seriously damaged and the dermis structure was disordered while some red blood cells and inflammatory cells exudated or infiltrated. Severe atrophy of the epidermis is characterized by monolayer cells with dermis structure disorder and no obvious red blood cell exudation and a small amount of inflammatory cell infiltration in APRFE group. Disappearance of epidermis is characterized by only monolayer cells with dermis disorder and no obvious red blood cell exudation, but a small amount of inflammatory cell infiltration in SVFG group. Severe atrophy of the epidermis in the SVFG combined with APRFE group showed monolayer or double-layer cells, dermis structure disorder, no obvious red blood cell exudation and a small amount of inflammatory cell infiltration.

On 14 d after intervention, in the control group, the epidermis was obviously thickened and the structure of dermis was disordered. There was no obvious exudation of red blood cells, and there was a small amount of inflammatory cell infiltration. In APRFE group, the epidermis partially recovered and the structure of dermis was disordered. There was no obvious exudation of red blood cells, and there was some inflammatory cell infiltration. In SVF group, the epidermis was partially recovered and the structure of dermis was partially disordered. There was no obvious erythrocyte exudation, and there was some inflammatory cell infiltration. The epidermis of the combined intervention group basically recovered, with partial thickening and dermis structure disorder, no obvious red blood cell exudation and some inflammatory cell infiltration.

On 28 d after intervention, in the control group, there were thickened epidermis, keratinization of multiple layers of cells and disordered arrangement of dermis, no obvious exudation of red blood cells and infiltration of some inflammatory cells. In APRFE group, there was no obvious change in epidermis and partial disorder of dermis, no obvious erythrocyte exudation and some inflammatory cell infiltration compared with 14 days. In SVFG group, the epidermis was thickened and the cells were keratinized,

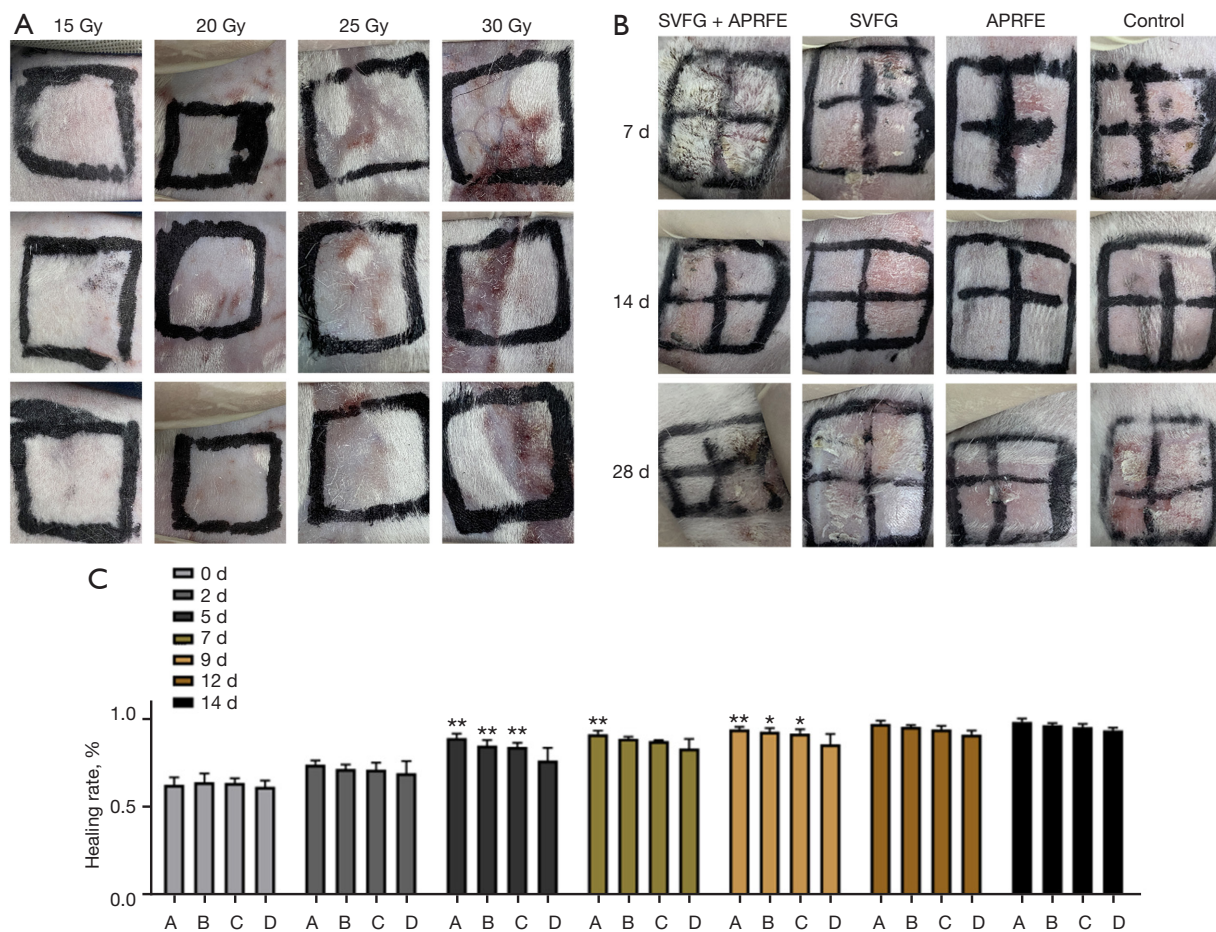


Figure 3 Animal irradiated model construction and intervention. (A) State of the pre-experimental 12 rabbits after being irradiated; (B) state of the rabbits in each group after intervention; (C) comparison of the wound healing rates in the four groups on 2, 5, 7, 9, 12 and 14 d after intervention. Group A: 0.3mL APRFE + 1 mL SVFG; group B: 1 mL SVFG; group C: 0.3 mL APRFE; group D: 1 mL NS. * $P < 0.05$, ** $P < 0.01$, compared with the control group. SVFG, stromal vascular fraction gel; APRFE, advanced platelet-rich fibrin extract; NS, normal saline.

the arrangement of dermis was disordered. There was no obvious exudation of red blood cells, and there was some inflammatory cell infiltration. In the combined intervention group, part of the epidermis thickened and the dermis was basically normal. There was no obvious red blood cell exudation and a small amount of inflammatory cell infiltration (Figure 4).

Masson staining

Masson results showed that after irradiation, the collagen content in the combined intervention group was significantly higher than that in the control group; the collagen content in the SVFG group and APRFE group

was significantly higher than that in the control group; the collagen content in the control group was the least. (** $P < 0.01$, compared with the control group; ## $P < 0.01$, compared with the APRFE group; & $P < 0.05$, compared with the SVFG group) (Figure 5).

IHC detection

The results of IHC showed that the expression of CD31 in the combined intervention group was significantly higher than that in the control group at each time point, and the highest expression was on the 14th day; the expression of CD31 in the SVFG group and the APRFE group were significantly higher than that in the control group on the

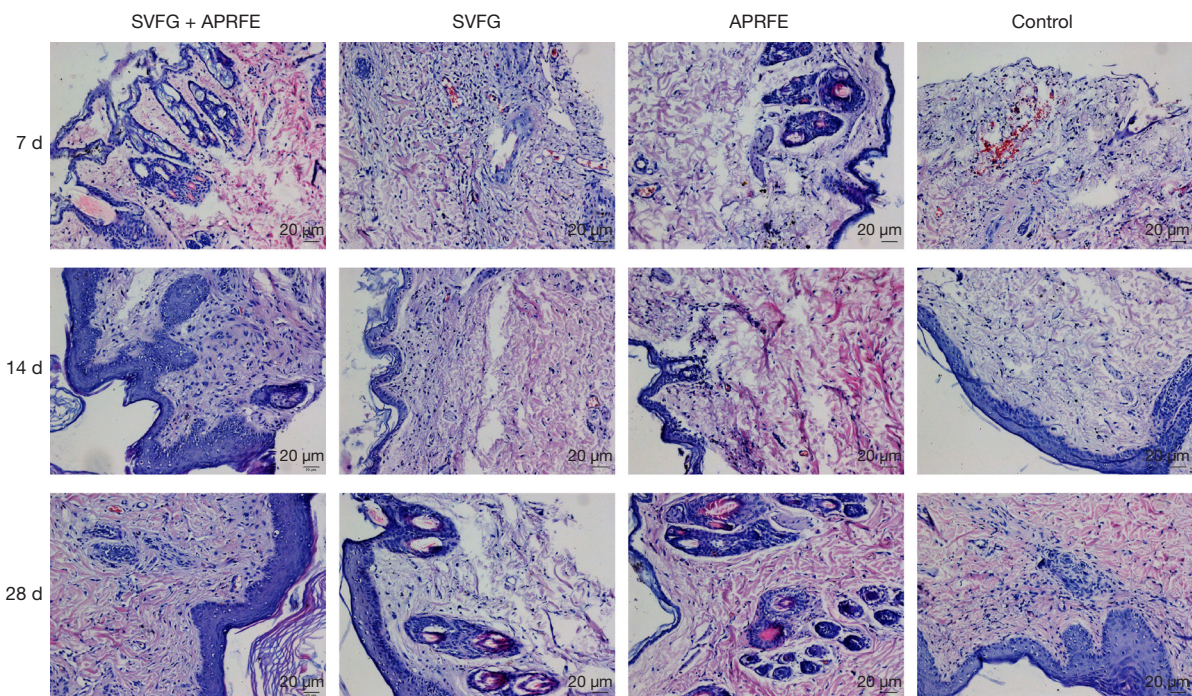


Figure 4 HE staining was performed on the corresponding wound samples in the four groups on 7, 14, and 28 d after intervention. Amplify $\times 100$. SVFG, stromal vascular fraction gel; APRFE, advanced platelet-rich fibrin extract; HE, hematoxylin and eosin.

7th and 14th day, there was no significant difference on the 28th day. The highest expression of CD31 SVFG group and the APRFE group were on the 14th day; the highest expression of CD31 was on the 28th day in the model group. (** $P < 0.01$, compared with the control group; # $P < 0.05$, ## $P < 0.01$, compared with the APRFE group; && $P < 0.01$, compared with the SVFG group) (Figure 6).

WB and RT-PCR analysis

The results of WB RT-PCR showed that the mRNA and protein expression levels of HIF-1 α , IL-10, K19 and VEGF in the combined treatment group were significantly higher than those in the control group, while those in the SVFG group and APRFE group were higher than those in the control group only at some time points; the protein expression level of IL-8 in the combined treatment group was significantly lower than those in the control group, while that in the SVFG and APRFE group were significantly lower than that in the control group at some time points. (* $P < 0.05$, ** $P < 0.01$, compared with the control group; # $P < 0.05$, ## $P < 0.01$, compared with the APRFE group; & $P < 0.05$, && $P < 0.01$, compared with the SVFG group) (Figures 7,8).

Discussion

The most important role of collagen in tissue regeneration and healing is to maintain the dynamic balance between synthesis and degradation. Felix RG reported that ADSCs and ADSCs-CM modulate an *in situ* imbalance between collagen I- and Col V-mediated IL-17 immune response (24), SVFG contains ADSCs, which can stimulate fibroblasts to synthesize a large amount of collagen cell matrix secretion after injection into the wounds. Fibroblasts are the main cells responsible for collagen synthesis, and the growth factors conducive to collagen fiber synthesis are mainly PDGF, TGF- β , IL-1, IL-4, TNF- α , etc. APRFE is enriched with growth factors and cytokines which were mentioned above and are helpful to reconstruct and repair the radiation injury of skin and soft tissue. In the process of wound repair, epidermal stem cells with positive expression of K19 were found in granulation tissue and other skin tissue structures, which are the basis of wound repair. In this study, K19 was found to be high expression in the combined treatment group, which indicated that high-spirited SVFG combined with APRFE promoting significant effect on radiation injury repair of skin and soft tissue.

The decrease of microvessel density in tissue after

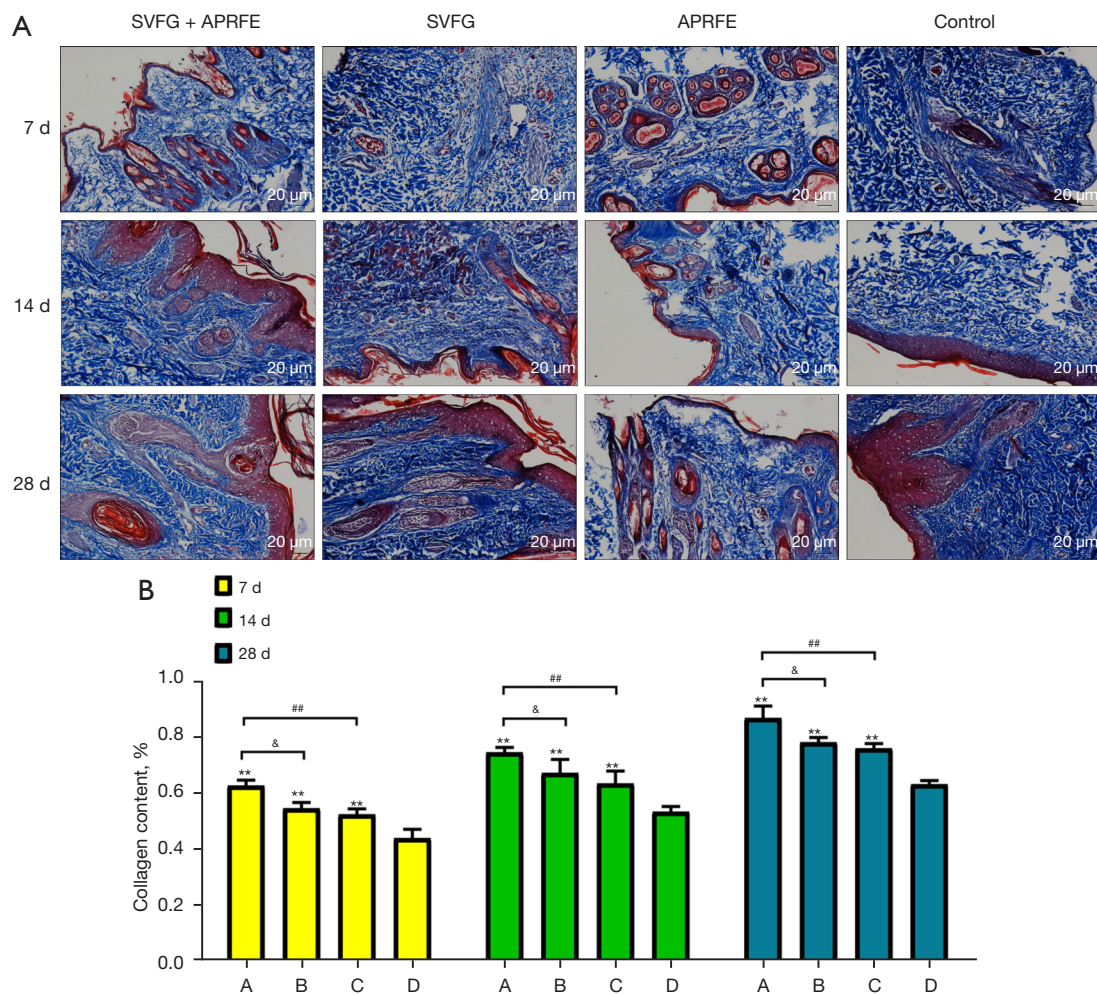


Figure 5 Masson staining and collagen detection. (A) The microscopic observation of corresponding wound samples after intervention were taken for Masson staining. Amplify $\times 100$. (B) The collagen content of each group was compared according to the results of Masson staining and presented it in the bar chart. Group A: 0.3 mL APRFE + 1 mL SVFG; group B: 1 mL SVFG; group C: 0.3 mL APRFE; group D: 1 mL NS. ** $P < 0.01$, compared with the control group; ## $P < 0.01$, compared with the APRFE group; & $P < 0.05$, compared with the SVFG group. SVFG, stromal vascular fraction gel; APRFE, advanced platelet-rich fibrin extract; NS, normal saline.

ionizing radiation leads to tissue ischemia, which is an important factor affecting injury wounds healing. In the this study, we found that highly purified SVFG combined with APRFE therapy is more effective in promoting neovascularization and tissue remodeling, which is more beneficial to the repair of radiation skin and soft tissue injury than single SVFG or APRFE group. CD31 as a specific marker of vascular endothelial cells, which was high expression and microvessel density increasing significantly in healing tissue of the combined treatment group after 2 weeks treatment. It is suggested that highly purified SVFG combined with APRFE can significantly promote

the angiogenesis of injured tissue and accelerate vascular reconstruction. Because angiogenesis is an important part of radiation injury repair, the injectable highly purified SVFG enriched with ADSCs have been confirmed to differentiate into vascular endothelial cells, smooth muscle cells, and pericytes, or directly participating in angiogenesis (25-27). Moreover, cytokines secreted by ADSCs and PDGF, VEGF, FGF-2, EGF, IGF and TGF- β in APRFE effectively promote neovascularization (28). Studies have shown that APRFE is beneficial for ADSCs to migrate to the injured area and the factors of TGF- β 1, VEGF and PDGF-AB contained in APRFE play an important role in

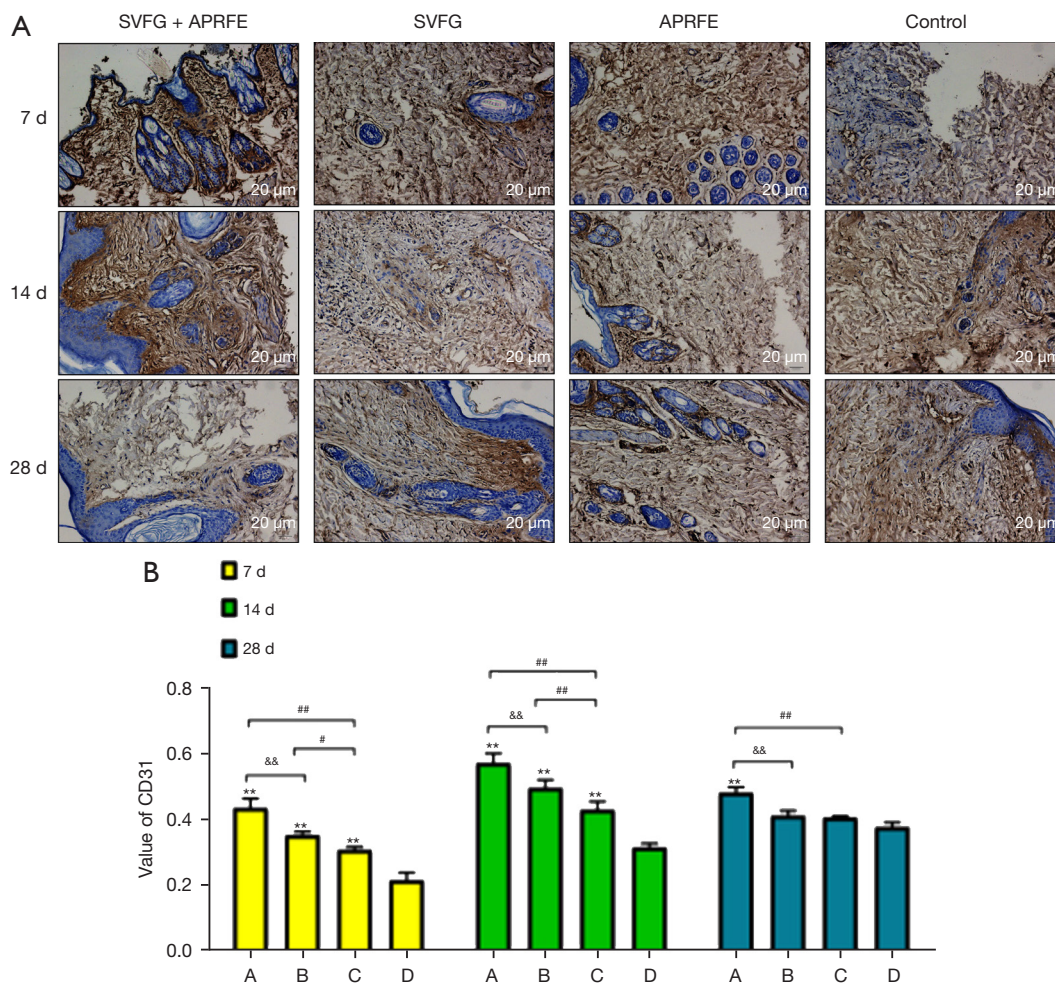


Figure 6 CD31 level in each wound tissue was analyzed by IHC staining. (A) Corresponding wound tissue after intervention was sampled for IHC analysis. Amplify $\times 100$. (B) The CD31 level of each group was presented in the bar chart. Group A: 0.3 mL APRFE + 1 mL SVFG; group B: 1 mL SVFG; group C: 0.3 mL APRFE; group D: 1 mL NS. ** $P < 0.01$, compared with the control group; # $P < 0.05$, ## $P < 0.01$, compared with the APRFE group; && $P < 0.01$, compared with the SVFG group. SVFG, stromal vascular fraction gel; APRFE, advanced platelet-rich fibrin extract; IHC, immunohistochemistry; NS, normal saline.

the adhesion, proliferation and differentiation of ADSCs via activating three pathways (tryptophan metabolism, mTOR signaling pathway, and adipocytokine signaling) (29,30). In addition, the three-dimensional APRF is an important structure for platelet concentrate to function. It can snare ADSCs and prevent cell loss, load platelets, leukocytes and cytokines, and provide space support for cell growth and proliferation (31,32).

Early revascularization provides a good microenvironment for tissue injury repair. The expression of pro-inflammatory factors such as TNF- α , IL-1 and IL-6 increased, and cell adhesion molecules were released at the same time, which

accelerated the migration, adhesion and exudation of leukocytes, and induced the migration of macrophages, neutrophils and monocytes to the wound surface, which resulting in local inflammatory reaction in the initial stage of radiation injury. ADSCs can down-regulate the expression of these pro-inflammatory cytokines and increase the secretion of anti-inflammatory factors such as IL-4 and IL-10, which regulate the inflammatory response by regulating the functions of macrophages, dendritic cells, T lymphocytes, B lymphocytes and natural killer cells (32-34). Studies have shown that PRF can continuously release a variety of growth factors that are beneficial to

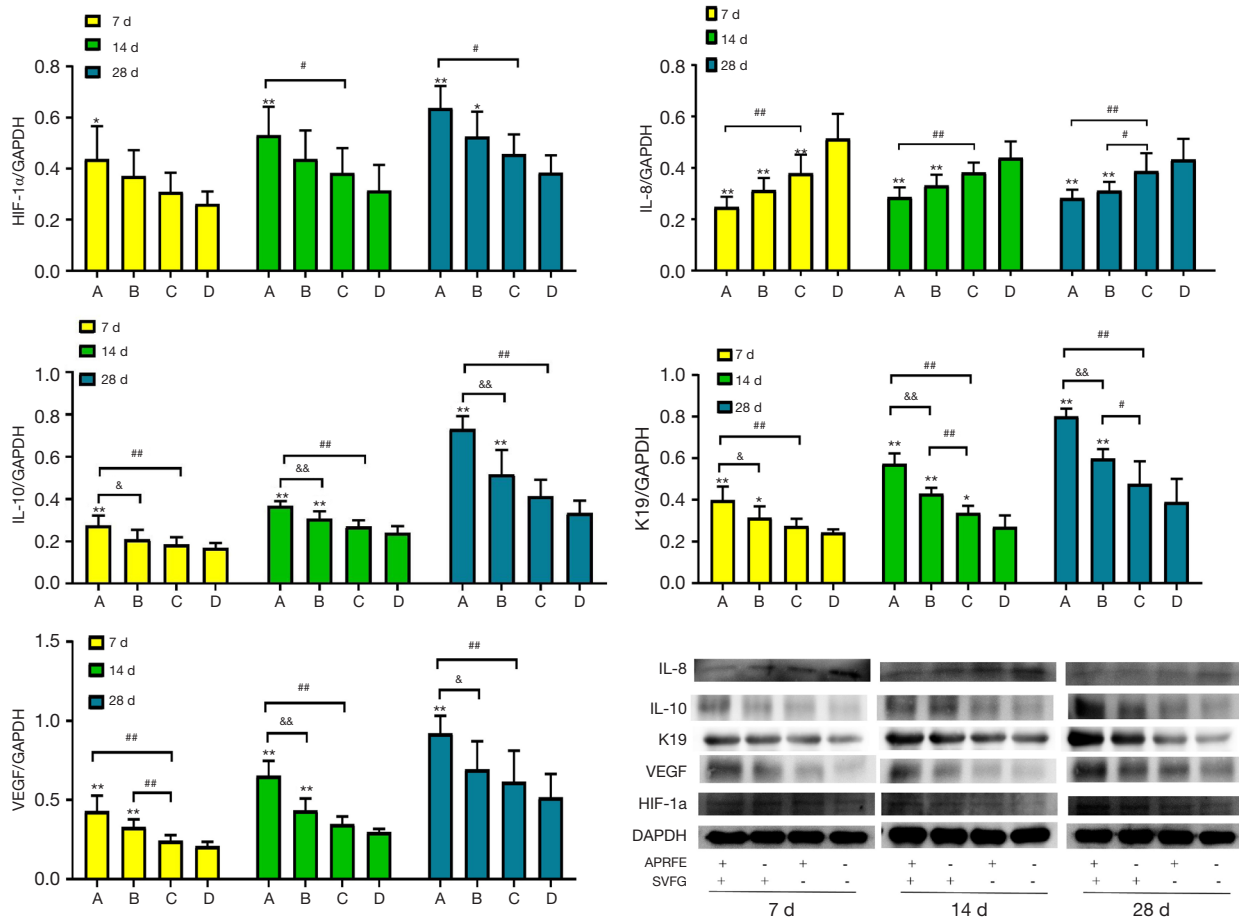


Figure 7 Western blot was performed for the respective wound samples to detect the expression level of each kind of protein. Group A: 0.3 mL APRFE + 1 mL SVFG; group B: 1 mL SVFG; group C: 0.3 mL APRFE; group D: 1 mL NS. * $P < 0.05$, ** $P < 0.01$, compared with the control group; # $P < 0.05$, ## $P < 0.01$, compared with the APRFE group; $\&P < 0.05$, $\&\&P < 0.01$, compared with the SVFG group. HIF-1 α , hypoxia inducible factor-1 α ; GAPDH, glyceraldehyde-3-phosphate dehydrogenase; IL-8, interleukin 8; IL-10, interleukin 10; VEGF, vascular endothelial growth factor; APRFE, advanced platelet-rich fibrin extract; SVFG, stromal vascular fraction gel; NS, normal saline.

wound healing; protecting them from proteolytic enzyme degradation; reducing local adverse immune reactions; decreasing the inflammatory response of mesenchymal cells and enhancing anti-infection ability (35,36). In this study, we found that high expression of IL-10 and low expression of IL-8 in highly purified SVFG combined with APRFE treatment group, indicating that SVFG and APRFE can effectively reduce inflammatory response, which is related to their paracrine function, providing a good microenvironment for radiation damage tissue repair and cell regeneration, which is conducive to the further reconstruction of early neovascularization network.

Ionizing radiation increases the release of reactive

oxygen species (ROS), nitric oxide and stress particles, causing microvascular damage, reducing tissue blood perfusion, and finally leading to local tissue hypoxia (37-39). ADSCs originates around the blood vessels of adipose tissue *in vivo*. This hypoxic growth environment makes ADSCs less metabolic and more adaptable to hypoxia caused by ionizing radiation. ADSCs can not only survive under hypoxia, but also exert its biological functions such as proliferation and paracrine, so hypoxia is commonly used to pretreat ADSCs (40-42). At the same time, tissue hypoxia can promote the high expression of HIF-1 α and stimulate the secretion of VEGF, FGF and HGF by ADSCs in SVFG, which contributes to angiogenesis and increases tissue

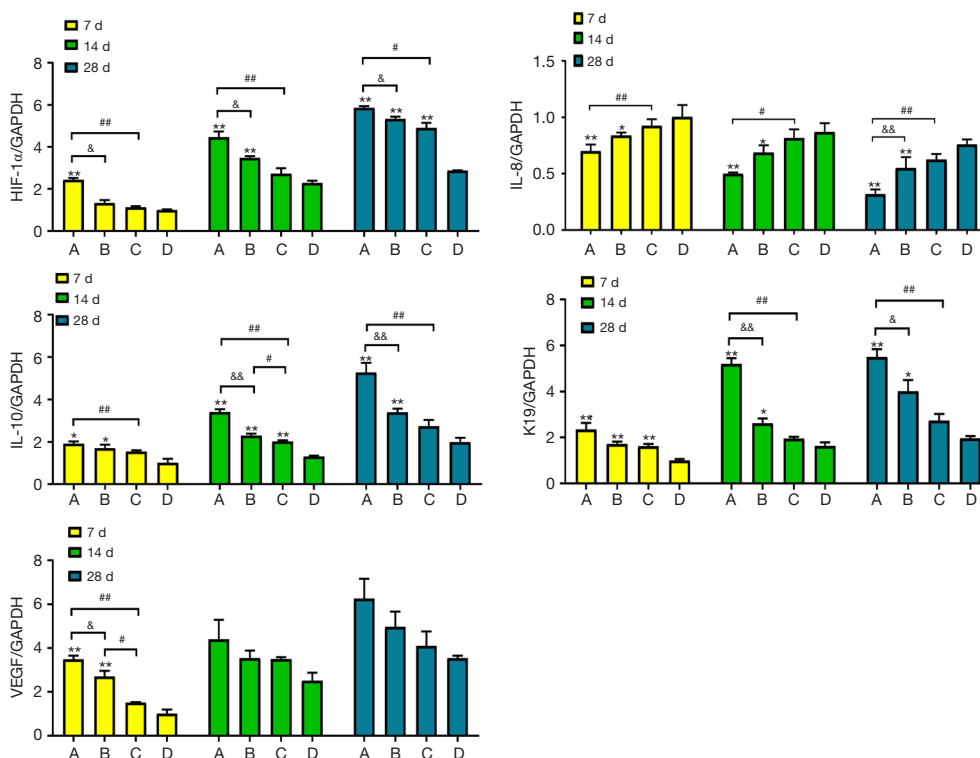


Figure 8 Wounds tissues in the four groups were sampled for RT-PCR to measure the level of each kind of mRNA expression. Group A: 0.3 mL APRFE + 1 mL SVFG; group B: 1 mL SVFG; group C: 0.3 mL APRFE; group D: 1.0 mL NS. * $P < 0.05$, ** $P < 0.01$, compared with the control group; # $P < 0.05$, ## $P < 0.01$, compared with the APRFE group; & $P < 0.05$, && $P < 0.01$, compared with the stromal SVFG group. HIF-1 α , hypoxia inducible factor-1 α ; GAPDH, glyceraldehyde-3-phosphate dehydrogenase; IL-8, interleukin 8; IL-10, interleukin 10; VEGF, vascular endothelial growth factor; RT-PCR, reverse transcription polymerase chain reaction detection; APRFE, advanced platelet-rich fibrin extract; SVFG, stromal vascular fraction gel; NS, normal saline.

oxygen content. The results of this study confirmed that highly purified SVFG combined with APRFE promoted the expression of HIF-1 α and made ADSCs in SVFG exert its biological function, thus optimizing the repair process of skin radiation damage.

Conclusions

SVFG is a cell cluster composed of allogeneic cells and does not need to be cultured and expanded *in vitro*. It can replace cultured and amplified ASCs as a new source of seed cells for cell transplantation after radiation injury of skin and soft tissue. Moreover, APRFE, which is enriched with a variety of growth factors, so it is easy to be used in clinical application, solving the nutritional problem for the regeneration and repair of radioactive skin and soft tissue. In summary, the intervention therapy of highly purified SVFG combined with APRFE mainly promotes the repair

of injured tissue by increasing the expression of HIF-1 α to stimulate angiogenesis, promoting the secretion of anti-inflammatory factors and reducing the secretion of pro-inflammatory factors, which provides a new treatment strategy for the repair of radiation injury of skin and soft tissue in clinic.

Acknowledgments

Funding: This work was supported by the Guangxi Natural Science Foundation of China (No. 2018GXNSFAA281148); the Youth Science Innovation and Entrepreneurship Talent Training Project of Nanning (No. RC20190206); the Scientific Research and Technology Development Program of Nanning Liangqing District (No. 202010); the Yong River Program of Innovation and Entrepreneurship of Nanning (No. 2018-01-07); the Guangxi Key Laboratory of Regenerative Medicine Open Fund Project Guangxi

Reopening (No. 202007); and the Self-Funded Scientific Research Project of Guangxi Zhuang Autonomous Region Health Commission (No. Z-A20220149).

Footnote

Reporting Checklist: The authors have completed the ARRIVE reporting checklist. Available at <https://atm.amegroups.com/article/view/10.21037/atm-22-3956/rc>

Data Sharing Statement: Available at <https://atm.amegroups.com/article/view/10.21037/atm-22-3956/dss>

Conflicts of Interest: All authors have completed the ICMJE uniform disclosure form (available at <https://atm.amegroups.com/article/view/10.21037/atm-22-3956/coif>). AL is from Guangxi Kangjiu Biotechnology Co., Ltd., Nanning and QH is from Nanning Wilking Biotechnology Co., Ltd., Nanning. The other authors have no conflicts of interest to declare.

Ethical Statement: The authors are accountable for all aspects of the work in ensuring that questions related to the accuracy or integrity of any part of the work are appropriately investigated and resolved. Animal experiments were performed under a project license (No. 2020-106-01) granted by the Ethics Committee of the Fifth Affiliated Hospital of Guangxi Medical University, in compliance with the institutional guidelines for the care and use of animals.

Open Access Statement: This is an Open Access article distributed in accordance with the Creative Commons Attribution-NonCommercial-NoDerivs 4.0 International License (CC BY-NC-ND 4.0), which permits the non-commercial replication and distribution of the article with the strict proviso that no changes or edits are made and the original work is properly cited (including links to both the formal publication through the relevant DOI and the license). See: <https://creativecommons.org/licenses/by-nc-nd/4.0/>.

References

- Zheng R, Zhang S, Zeng H, et al. Cancer incidence and mortality in China, 2016. *Journal of the National Cancer Center* 2022;102:1987-92.
- Borrelli MR, Shen AH, Lee GK, et al. Radiation-Induced Skin Fibrosis: Pathogenesis, Current Treatment Options, and Emerging Therapeutics. *Ann Plast Surg* 2019;83:S59-64.
- Adem S, Abbas DB, Lavin CV, et al. Decellularized Adipose Matrices Can Alleviate Radiation-Induced Skin Fibrosis. *Adv Wound Care (New Rochelle)* 2022;11:524-36.
- Evin N, Tosun Z, Aktan TM, et al. Effects of Adipose-Derived Stem Cells and Platelet-Rich Plasma for Prevention of Alopecia and Other Skin Complications of Radiotherapy. *Ann Plast Surg* 2021;86:588-97.
- Lee J, Jang H, Park S, et al. Platelet-rich plasma activates AKT signaling to promote wound healing in a mouse model of radiation-induced skin injury. *J Transl Med* 2019;17:295.
- Soriano JL, Calpena AC, Souto EB, et al. Therapy for prevention and treatment of skin ionizing radiation damage: a review. *Int J Radiat Biol* 2019;95:537-53.
- Sheykhasan M, Wong JKL, Seifalian AM. Human Adipose-Derived Stem Cells with Great Therapeutic Potential. *Curr Stem Cell Res Ther* 2019;14:532-48.
- Hou X, Wang Z, Ding F, et al. Taurine Transporter Regulates Adipogenic Differentiation of Human Adipose-Derived Stem Cells through Affecting Wnt/ β -catenin Signaling Pathway. *Int J Biol Sci* 2019;15:1104-12.
- Luo Y, Ge R, Wu H, et al. The osteogenic differentiation of human adipose-derived stem cells is regulated through the let-7i-3p/LEF1/ β -catenin axis under cyclic strain. *Stem Cell Res Ther* 2019;10:339.
- Keshavarz G, Jalili C, Pazhouhi M, et al. Resveratrol Effect on Adipose-Derived Stem Cells Differentiation to Chondrocyte in Three-Dimensional Culture. *Adv Pharm Bull* 2020;10:88-96.
- Arderiu G, Peña E, Aledo R, et al. MicroRNA-145 Regulates the Differentiation of Adipose Stem Cells Toward Microvascular Endothelial Cells and Promotes Angiogenesis. *Circ Res* 2019;125:74-89.
- Yu D, Zhang S, Mo W, et al. Transplantation of the Stromal Vascular Fraction (SVF) Mitigates Severe Radiation-Induced Skin Injury. *Radiat Res* 2021;196:250-60.
- Stachura A, Paskal W, Pawlik W, et al. The Use of Adipose-Derived Stem Cells (ADSCs) and Stromal Vascular Fraction (SVF) in Skin Scar Treatment-A Systematic Review of Clinical Studies. *J Clin Med* 2021;10:3637.
- Deng C, Wang L, Feng J, et al. Treatment of human chronic wounds with autologous extracellular matrix/stromal vascular fraction gel: A STROBE-compliant study. *Medicine (Baltimore)* 2018;97:e11667.
- Ghanaati S, Booms P, Orlowska A, et al. Advanced platelet-rich fibrin: a new concept for cell-based tissue

- engineering by means of inflammatory cells. *J Oral Implantol* 2014;40:679-89.
16. Liu B, Tan XY, Liu YP, et al. The adjuvant use of stromal vascular fraction and platelet-rich fibrin for autologous adipose tissue transplantation. *Tissue Eng Part C Methods* 2013;19:1-14.
 17. Zhai Z, Yu P, Huang M, et al. Comparison Effects of Platelet-Rich Fibrin on Macrolipid and Shuffling Fat Grafting. *J Craniofac Surg* 2019;30:2332-6.
 18. Xiong S, Qiu L, Su Y, et al. Platelet-Rich Plasma and Platelet-Rich Fibrin Enhance the Outcomes of Fat Grafting: A Comparative Study. *Plast Reconstr Surg* 2019;143:1201e-12e.
 19. Carstens MH, Zelaya M, Calero D, et al. Adipose-derived stromal vascular fraction (SVF) cells for the treatment of non-reconstructable peripheral vascular disease in patients with critical limb ischemia: A 6-year follow-up showing durable effects. *Stem Cell Res* 2020;49:102071.
 20. Bi H, Li H, Zhang C, et al. Stromal vascular fraction promotes migration of fibroblasts and angiogenesis through regulation of extracellular matrix in the skin wound healing process. *Stem Cell Res Ther* 2019;10:302.
 21. Liang Z, Huang D, Nong W, et al. Advanced-platelet-rich fibrin extract promotes adipogenic and osteogenic differentiation of human adipose-derived stem cells in a dose-dependent manner in vitro. *Tissue Cell* 2021;71:101506.
 22. Liu Y, Sun X, Yu J, et al. Platelet-Rich Fibrin as a Bone Graft Material in Oral and Maxillofacial Bone Regeneration: Classification and Summary for Better Application. *Biomed Res Int* 2019;2019:3295756.
 23. Amaral Valladao CA Jr, Freitas Monteiro M, Joly JC. Guided bone regeneration in staged vertical and horizontal bone augmentation using platelet-rich fibrin associated with bone grafts: a retrospective clinical study. *Int J Implant Dent* 2020;6:72.
 24. Felix RG, Bovolato ALC, Cotrim OS, et al. Adipose-derived stem cells and adipose-derived stem cell-conditioned medium modulate in situ imbalance between collagen I- and collagen V-mediated IL-17 immune response recovering bleomycin pulmonary fibrosis. *Histol Histopathol* 2020;35:289-301.
 25. Parshyna I, Lehmann S, Grahl K, et al. Impact of omega-3 fatty acids on expression of angiogenic cytokines and angiogenesis by adipose-derived stem cells. *Atheroscler Suppl* 2017;30:303-10.
 26. Zheng H, Qiu L, Su Y, et al. Conventional Nanofat and SVF/ADSC-Concentrated Nanofat: A Comparative Study on Improving Photoaging of Nude Mice Skin. *Aesthet Surg J* 2019;39:1241-50.
 27. Xiao S, Deng Y, Mo X, et al. Promotion of Hair Growth by Conditioned Medium from Extracellular Matrix/Stromal Vascular Fraction Gel in C57BL/6 Mice. *Stem Cells Int* 2020;2020:9054514.
 28. Chen B, Sun HH, Wang HG, et al. The effects of human platelet lysate on dental pulp stem cells derived from impacted human third molars. *Biomaterials* 2012;33:5023-35.
 29. Thanasrisuebwong P, Kiattavorncharoen S, Surarit R, et al. Red and Yellow Injectable Platelet-Rich Fibrin Demonstrated Differential Effects on Periodontal Ligament Stem Cell Proliferation, Migration, and Osteogenic Differentiation. *Int J Mol Sci* 2020;21:5153.
 30. Lu GM, Jiang LY, Huang DL, et al. Advanced platelet-rich fibrin extract treatment promotes the proliferation and differentiation of Human Adipose-Derived Mesenchymal Stem Cells through activation of tryptophan metabolism. *Curr Stem Cell Res Ther* 2021. [Epub ahead of print]. doi: 10.2174/1574888X16666211206150934.
 31. Dohan Ehrenfest DM, Del Corso M, Diss A, et al. Three-dimensional architecture and cell composition of a Choukroun's platelet-rich fibrin clot and membrane. *J Periodontol* 2010;81:546-55.
 32. Borrelli MR, Patel RA, Adem S, et al. The antifibrotic adipose-derived stromal cell: Grafted fat enriched with CD74+ adipose-derived stromal cells reduces chronic radiation-induced skin fibrosis. *Stem Cells Transl Med* 2020;9:1401-13.
 33. Ortiz-Virumbrales M, Menta R, Pérez LM, et al. Human adipose mesenchymal stem cells modulate myeloid cells toward an anti-inflammatory and reparative phenotype: role of IL-6 and PGE2. *Stem Cell Res Ther* 2020;11:462.
 34. Heidari N, Abbasi-Kenarsari H, Namaki S, et al. Adipose-derived mesenchymal stem cell-secreted exosome alleviates dextran sulfate sodium-induced acute colitis by Treg cell induction and inflammatory cytokine reduction. *J Cell Physiol* 2021;236:5906-20.
 35. Wang J, Xiang B, Deng JX, et al. Hypoxia enhances the therapeutic potential of superparamagnetic iron oxide-labeled adipose-derived stem cells for myocardial infarction. *J Huazhong Univ Sci Technolog Med Sci* 2017;37:516-22.
 36. Kargarpour Z, Nasirzade J, Panahipour L, et al. Platelet-Rich Fibrin Decreases the Inflammatory Response of Mesenchymal Cells. *Int J Mol Sci* 2021;22:11333.
 37. Du Z, Liu H, Huang X, et al. Design and Synthesis of a

- Mitochondria-Targeting Radioprotectant for Promoting Skin Wound Healing Combined with Ionizing Radiation Injury. *Pharmaceuticals (Basel)* 2022;15:721.
38. Filimonova M, Saburova A, Makarchuk V, et al. The Ability of the Nitric Oxide Synthases Inhibitor T1023 to Selectively Protect the Non-Malignant Tissues. *Int J Mol Sci* 2021;22:9340.
 39. Konieczny P, Xing Y, Sidhu I, et al. Interleukin-17 governs hypoxic adaptation of injured epithelium. *Science* 2022;377:eabg9302.
 40. Choi JW, Moon H, Jung SE, et al. Hypoxia Rapidly Induces the Expression of Cardiomyogenic Factors in Human Adipose-Derived Adherent Stromal Cells. *J Clin Med* 2019;8:1231.
 41. Rashidbenam Z, Jasman MH, Tan GH, et al. Fabrication of Adipose-Derived Stem Cell-Based Self-Assembled Scaffold under Hypoxia and Mechanical Stimulation for Urethral Tissue Engineering. *Int J Mol Sci* 2021;22:3350.
 42. Huang H, Tang X, Li S, et al. Advanced platelet-rich fibrin promotes the paracrine function and proliferation of adipose-derived stem cells and contributes to micro-autologous fat transplantation by modulating HIF-1 α and VEGF. *Ann Transl Med* 2022;10:60.

(English Language Editor: J. Jones)

Cite this article as: Li Z, Gan H, Liang A, Wang X, Hu X, Liang P, Xu G, Huang Q, Li J, Li H. Promoting repair of highly purified stromal vascular fraction gel combined with advanced platelet-rich fibrin extract for irradiated skin and soft tissue injury. *Ann Transl Med* 2022;10(17):933. doi: 10.21037/atm-22-3956